EUROPEAN LABORATORY FOR PARTICLE PHYSICS

CERN/PS/90-53 (OP)
26 July 1990

Transition Revisited

Steve Hancock

Abstract

The standard derivations of the energy and phase of the synchronous particle in a proton accelerator assume, as if by definition, that said synchronous particle lies on the central orbit of the machine. This is manifestly unjustified in the particular case of the acceleration near transition of a mixture of ions, when a small difference in charge-to-mass ratio can produce a large radial separation of the different ion species.

The development of a simple derivation of the parameters of the synchronous particle that involves no such *a priori* constraint has yielded some surprises; not least, a belated explanation for an apparent anomaly encountered in 1987, when a mixture of oxygen and sulphur ions was accelerated in the PS for the first time. These ideas are supported by measurements performed during the latest ion run.

Geneva, Switzerland.

1 PREAMBLE

In the autumn of 1987, sulphur ions were accelerated at CERN to a world-record energy of 6.4 TeV. The $^{32}S^{16+}$ ions were supplied by an electron cyclotron resonance source which, for reasons principally pertaining to electron stripping efficiency, also produced $^{16}O^{8+}$ ions. Significantly, however, the oxygen ions constituted a ninety percent "contamination" of the total beam current. Since the relative charge-to-mass ratio difference of $^{16}O^{8+}$ with respect to $^{32}S^{16+}$ is only about -5.4×10^{-4}, the oxygen was essentially indistinguishable from sulphur throughout the acceleration process, with the exception of the region near transition. It was near transition in the PS that the oxygen was eliminated.

The slight difference in charge-to-mass ratio enables one beam to be attributed an effective relative momentum defect with respect to the synchronous particle of the other type and, near transition, the importance of a momentum defect becomes magnified. Therefore, in the adiabatic limit, the result at transition should be an infinitely large radial separation of the two ion species.

Thus, it was reasoned, an RF beam control system which maintained sulphur near the central orbit would bring about the demise of the oxygen ions against the outer wall of the vacuum chamber when transition was crossed, particularly if the so-called γ_{tr}-jump were disabled in order to approach more closely the adiabatic limit. Likewise, if the RF system were set up to maintain the synchronous particle for oxygen near the centre of the aperture, the sulphur ions would be lost against the inner wall of the vacuum chamber.

In practice, only the latter was observed; the oxygen could not be completely eliminated without the *ad hoc* addition of a small perturbation to the RF phase programme a few tens of milliseconds before the phase jump at transition. (The beam control system only involved a phase loop.) This perturbation had the effect of driving both beams towards the outside of the machine, so that the oxygen was removed leaving sulphur to cross transition alone.

The "asymmetry" of the selection process could not be satisfactorily explained. Despite the glaringly obvious fact of the beam control system being dominated by the oxygen, there seemed to be no convincing mechanism to cause an RF system which included no radial feedback to behave differently in the two cases.

2 THE SYNCHRONOUS PARTICLE

2.1 The "Standard Creed"

The standard derivations of the energy and phase of the synchronous particle in a proton accelerator assume, as if by definition, that said synchronous particle lies on the central orbit of the machine. However, this requires that the accelerating RF system acts in such a way as to justify the assumption. Usually, the RF system includes a radial feedback loop and the assumption is indeed valid, but at very low beam intensities, when it is difficult to make a reliable measurement of transverse position, successful acceleration depends upon the accuracy of the RF frequency programme.

The (angular) frequency which assures that a proton of speed $\beta_{\mathrm{nom}}c$ is synchronous on an orbit of mean radius R_{nom} is simply

$$\omega_{\mathrm{RF}} = \frac{h\beta_{\mathrm{nom}}c}{R_{\mathrm{nom}}}$$

where c is the speed of light *in vacuo* and the harmonic number, h, may be any positive integer (such that $\omega_{\rm RF}$ lies within the tunable range of the accelerating cavities). The momentum of this particle is given by the fundamental guide field relation

$$p_{\rm nom} = q_{\rm p} B_z \rho_{\rm nom} \tag{1}$$

Here, $q_{\rm p}$ is the proton's charge and $\rho_{\rm nom}$ is its radius of curvature in the dipole magnetic field, B_z, of the machine. Hence, eliminating $\beta_{\rm nom}$,

$$\omega_{\rm RF}(B_z) = \frac{hc}{R_{\rm nom}} \left[1 + \left(\frac{E_{\rm rest,p}}{q_{\rm p} B_z \rho_{\rm nom} c} \right)^2 \right]^{-1/2} \tag{2}$$

since $p_{\rm nom}c = E_{\rm rest,p}(\beta_{\rm nom}^{-2} - 1)^{-1/2}$, where $E_{\rm rest,p}$ is the rest-mass energy of the proton.

Taking the suffix nom to denote parameters which pertain to the central orbit, equation (2) describes the ideal RF frequency programme for protons. Provided that such a programme can be generated, equation (1) then gives the (total) energy of the synchronous particle as

$$E_{\rm nom} = \left[(q_{\rm p} B_z \rho_{\rm nom} c)^2 + E_{\rm rest,p}^2 \right]^{1/2} \tag{3}$$

Also, putting $E_{\rm nom} = E_{\rm tr} = \gamma_{\rm tr} E_{\rm rest,p}$, transition is found to occur when the magnetic field reaches a value of

$$B_{z,\rm tr} = \frac{E_{\rm rest,p}}{q_{\rm p} \rho_{\rm nom} c} (\gamma_{\rm tr}^2 - 1)^{1/2}$$

($E_{\rm tr}$ is the transition energy of the proton machine.)

The phase of the synchronous particle is commonly obtained by equating the energy gained by a proton in the accelerating electric field of the cavities to the work performed upon it per turn. Thus, again assuming that an ideal RF system maintains the synchronous particle on the central orbit, the synchronous phase (with respect to the zero-crossing of the RF), $\varphi_{\rm nom}$, is given by

$$q_{\rm p} \hat{V}_{\rm RF} \sin \varphi_{\rm nom} = \oint \frac{dp_{\rm nom}}{dt} d\ell$$

where $\hat{V}_{\rm RF}$ is the total (peak) RF voltage, ℓ is the distance along the particle's orbit and t is time. Hence

$$\sin \varphi_{\rm nom} = \frac{2\pi R_{\rm nom} \rho_{\rm nom}}{\hat{V}_{\rm RF}} \frac{dB_z}{dt} \tag{4}$$

assuming the variation of dB_z/dt during one turn to be negligible.

2.2 An Alternative Approach

Not unlike the "standard creed", I shall take the synchronous particle to be entirely defined by the free parameters of the magnetic field and the accelerating RF. But, initially at least, I shall make no assumptions about the form of the latter.

I begin by considering the so-called momentum compaction factor. This is defined

$$\alpha = \frac{p}{R} \left(\frac{\partial R}{\partial p} \right)_B$$

where the suffix B indicates that the derivative of mean orbital radius with respect to particle momentum excludes any contribution due to a time-variation of the magnetic field. Taking α to be independent of radial position (an assumption which is discussed in the following section), integration of this expression produces logarithmic terms in R and p and an integration constant that may be evaluated using equation (1) as a boundary condition at $R = R_{\rm nom}$. This yields

$$p = q_{\rm p} B_z \rho_{\rm nom} \left(\frac{R}{R_{\rm nom}} \right)^{1/\alpha} \tag{5}$$

Strictly, this is not the complete relationship between the mean radial position of a general proton and its momentum since it neglects the inertia that a real particle would exhibit in a changing magnetic field. However, I maintain that the synchronous particle is an ethereal creature and, as such, obeys the relationship not just at constant field, but at any instantaneous value of B_z. Furthermore, since the revolution frequency of the synchronous particle is $\omega_{\rm RF}/h$ (by definition), the synchronous orbit has $R_0 = h\beta_0 c/\omega_{\rm RF}$ and I write

$$\beta_0 E_0 = q_{\rm p} B_z \rho_{\rm nom} c \left(\frac{h\beta_0 c}{\omega_{\rm RF} R_{\rm nom}} \right)^{1/\alpha}$$

denoting the synchronous particle by suffix zero. Eliminating $\beta_0 = [1-(E_{\rm rest,p}/E_0)^2]^{1/2}$, the energy, E_0, of the synchronous particle is obtained by solving

$$E_0 (E_0^2 - E_{\rm rest,p}^2)^{(\alpha-1)/2} - \frac{hc}{\omega_{\rm RF} R_{\rm nom}} (q_{\rm p} B_z \rho_{\rm nom} c)^{\alpha} = 0 \tag{6}$$

In order to determine the synchronous phase, I consider the equation of motion of a general proton moving at radial position r about its own particular closed orbit (of mean radius R). Neglecting radiation losses, the azimuthal component of the Lorentz force equation is

$$\frac{1}{r} \frac{d(rp)}{dt} = q_{\rm p} \left(\hat{\mathcal{E}}_{\rm RF} \sin\varphi + \mathcal{E}_\theta + B_r \frac{dz}{dt} - B_z \frac{dr}{dt} \right) \tag{7}$$

where $\mathcal{E}_{\rm RF} = \hat{\mathcal{E}}_{\rm RF} \sin\omega_{\rm RF} t$ is the accelerating electric field, φ is the phase of the particle with respect to the zero-crossing of the same and where $\mathcal{E}_\theta$ is the azimuthal component of the electric field, $\underline{\mathcal{E}}$, which is produced in accordance with Faraday's Law by the time-variation of the magnetic field, $\underline{B} = (B_r, B_\theta, B_z)$. That is,

$$\oint \underline{\mathcal{E}}.d\underline{\ell} = -\frac{\partial}{\partial t} \int_S \underline{B}.d\underline{S}$$

where S is any surface that has the particle's orbit, ℓ, as its boundary. Making the "smooth" approximation that $\underline{B} = (<B_r>, 0, <B_z>)$, the angular brackets denoting the average around one turn of a circular machine, and noting that the energy gain per turn provided by the accelerating RF is independent of radial position, equation (7) becomes

$$\frac{1}{r} \frac{d(rp)}{dt} = q_{\rm p} \left(\frac{\hat{V}_{\rm RF}}{2\pi r} \sin\varphi + \mathcal{E}_\theta + <B_r> \frac{dz}{dt} - <B_z> \frac{dr}{dt} \right)$$

For the synchronous particle, this gives

$$p_0 \frac{dR_0}{dt} + R_0 \frac{dp_0}{dt} = \frac{q_{\rm p} \hat{V}_{\rm RF}}{2\pi} \sin\varphi_0 + q_{\rm p} R_0 \mathcal{E}_\theta(R_0) - q_{\rm p} R_0 \left(\frac{-p_0}{q_{\rm p} R_0} \right) \frac{dR_0}{dt}$$

by virtue of the more rigorous form of the fundamental guide field relation

$$<B_z>_{r=R_0} = -\frac{p_0}{q_p R_0}$$

(Cf. equation (1).) The minus sign enters here due to the fact that, in a right-handed cylindrical coordinate system, a positively charged particle moves in the negative θ-direction in a positive B_z-field. Hence

$$\sin\varphi_0 = \frac{2\pi R_0}{q_p \hat{V}_{RF}} \left(\frac{dp_0}{dt} + q_p \mathcal{E}_\theta(R_0) \right)$$

Or, since $d(p_0 c) = \beta_0^{-1} dE_0$,

$$\sin\varphi_0 = \frac{2\pi h}{q_p \hat{V}_{RF} \omega_{RF}} \frac{dE_0}{dt} + \frac{2\pi R_0}{\hat{V}_{RF}} \mathcal{E}_\theta(R_0) \tag{8}$$

2.2.1 An Aside on the values of α and $\mathcal{E}_\theta$

The momentum compaction factor is related to another, mercifully nameless parameter

$$\eta = \frac{p}{\omega_{rev}} \left(\frac{\partial \omega_{rev}}{\partial p} \right)_B$$

where ω_{rev} is the (angular) azimuthal revolution frequency of a particle of momentum p. Now,

$$\begin{aligned} \frac{d\omega_{rev}}{\omega_{rev}} &= \frac{d\beta}{\beta} - \frac{dR}{R}, \text{ since } \omega_{rev} = \beta c / R \\ &= \frac{1}{\gamma^2} \frac{dp}{p} - \frac{dR}{R}, \text{ since } \frac{dp}{p} = \frac{d\beta}{\beta} + \frac{d\gamma}{\gamma} = \gamma^2 \frac{d\beta}{\beta} \\ \Rightarrow \qquad \eta &= \frac{1}{\gamma^2} - \alpha, \text{ from the definition of } \alpha \end{aligned}$$

Hence, since the transition energy may be defined as that at which $\eta = 0$,

$$\alpha = \frac{1}{\gamma_{tr}^2}$$

The momentum compaction factor may also be expressed as an expansion in powers of the relative momentum defect with respect to the synchronous particle, i.e.,

$$\alpha = \alpha_0 + \alpha_1 \left(\frac{\Delta p}{p_0} \right) + \alpha_2 \left(\frac{\Delta p}{p_0} \right)^2 + \ldots$$

with $\Delta p = p - p_0$. Here, the higher order terms are a statement of the variation of γ_{tr} with particle momentum (or with mean orbital radius). However, γ_{tr} is closely related to the tune of the machine, so that these higher order terms are governed by the chromaticity. For transverse stability reasons, the chromaticity is ideally made to change sign at transition, but in practice its value is poorly known in this region. I shall assume that the chromaticity is sufficiently close to zero to enable me to neglect all terms higher than α_0. Thus, I shall take α to be independent of R.

In addition, I shall neglect the second term of equation (8) since the so-called betatron contribution, $2\pi R_0 \mathcal{E}_\theta(R_0)$, to the accelerating voltage per turn on the synchronous particle orbit is small beer indeed compared with $\hat{V}_{RF}$. There should even be no contribution at all on the central orbit of the PS because the number of magnet return yokes situated on the inside of the machine is matched by the number on the outside. Elsewhere, the betatron electric field is determined by the magnetic flux between R_0 and R_{nom} and is readily estimated to provide less than one volt per turn per millimetre between these orbits throughout any cycle in the PS repertoire.

2.2.2 The Special Case of an Ideal RF Frequency Programme

When equation (2) applies, the synchronous energy is obtained from a modified equation (6) which I choose to write

$$f_1(E_0) = f_2(B_z) \tag{9}$$

where

$$f_1(E_0) = q_p^{-1/\gamma_{tr}^2} E_0 (E_0^2 - E_{rest,p}^2)^{-(1-1/\gamma_{tr}^2)/2}$$

and

$$f_2(B_z) = (B_z \rho_{nom} c)^{1/\gamma_{tr}^2} \left[1 + \left(\frac{E_{rest,p}}{q_p B_z \rho_{nom} c} \right)^2 \right]^{1/2}$$

Now, since equation (9) is not particularly amenable to a closed-form solution, I should consider the form of f_1 and f_2 in an attempt to glean some physics insight before wading into a numerical analysis. These functions are plotted in figure 1 taking the central orbit parameters of the PS and a constant value of γ_{tr}. Assuming γ_{tr} to be invariant in time, i.e., in the absence of a γ_{tr}-jump, I note that

$$\begin{aligned}
f_1'(E_0) = 0 \quad &\Rightarrow \quad 0 = \frac{d}{dE_0} \left[E_0^2 (E_0^2 - E_{rest,p}^2)^{-(1-1/\gamma_{tr}^2)} \right], \text{ since } f_1(E_0) \neq 0 \\
&\Rightarrow \quad 0 = 2E_0^{-1} - \left(1 - \frac{1}{\gamma_{tr}^2} \right) (E_0^2 - E_{rest,p}^2)^{-1} 2E_0 \\
&\Rightarrow \quad E_0 = \gamma_{tr} E_{rest,p} \\
&\qquad\quad = E_{tr}
\end{aligned}$$

And

$$\begin{aligned}
f_2'(B_z) = 0 \quad &\Rightarrow \quad 0 = \frac{d}{dB_z} \left[B_z^{2/\gamma_{tr}^2} \left(1 + \left(\frac{E_{rest,p}}{q_p \rho_{nom} c} \right)^2 B_z^{-2} \right) \right], \text{ since } f_2(B_z) \neq 0 \\
&\qquad\quad = \frac{2}{\gamma_{tr}^2} B_z^{-(1-2/\gamma_{tr}^2)} - \left(2 - \frac{2}{\gamma_{tr}^2} \right) \left(\frac{E_{rest,p}}{q_p \rho_{nom} c} \right)^2 B_z^{-(1-2/\gamma_{tr}^2)-2} \\
&\Rightarrow \quad B_z = \frac{E_{rest,p}}{q_p \rho_{nom} c} (\gamma_{tr}^2 - 1)^{1/2} \\
&\qquad\quad = B_{z,tr}
\end{aligned}$$

Whence,

$$f_1(E_{tr}) = f_2(B_{z,tr})$$

Thus, the minima of f_1 and f_2 are associated with transition.

Furthermore, since each value of f_1 corresponds to two values of E_0 and each value of f_2 to two of B_z, solutions of equation (9) necessarily come in pairs. It is tempting to associate the synchronous energy solution below transition uniquely with the corresponding value of the magnetic field below $B_{z,tr}$ and the higher energy solution with the higher field, but this is not mathematically obvious. Nor is there any physical reason to dismiss one solution of each pair for, at given B_z, a particle can attain synchronism with ω_{RF} either by travelling at low speed on an orbit of small radius ($E_0 < E_{tr}$) or by travelling at higher speed on a larger orbit ($E_0 > E_{tr}$). Likewise, a particle of given energy can be synchronous either by moving on an orbit of large radius at a low revolution frequency

($B_z < B_{z,\mathrm{tr}}$) or by moving on a smaller orbit at a higher revolution frequency ($B_z > B_{z,\mathrm{tr}}$). Thus, choosing B_z as the free variable, equation (9) yields two solutions for E_0 on opposite sides of transition which approach each other as $B_z \to B_{z,\mathrm{tr}}$.

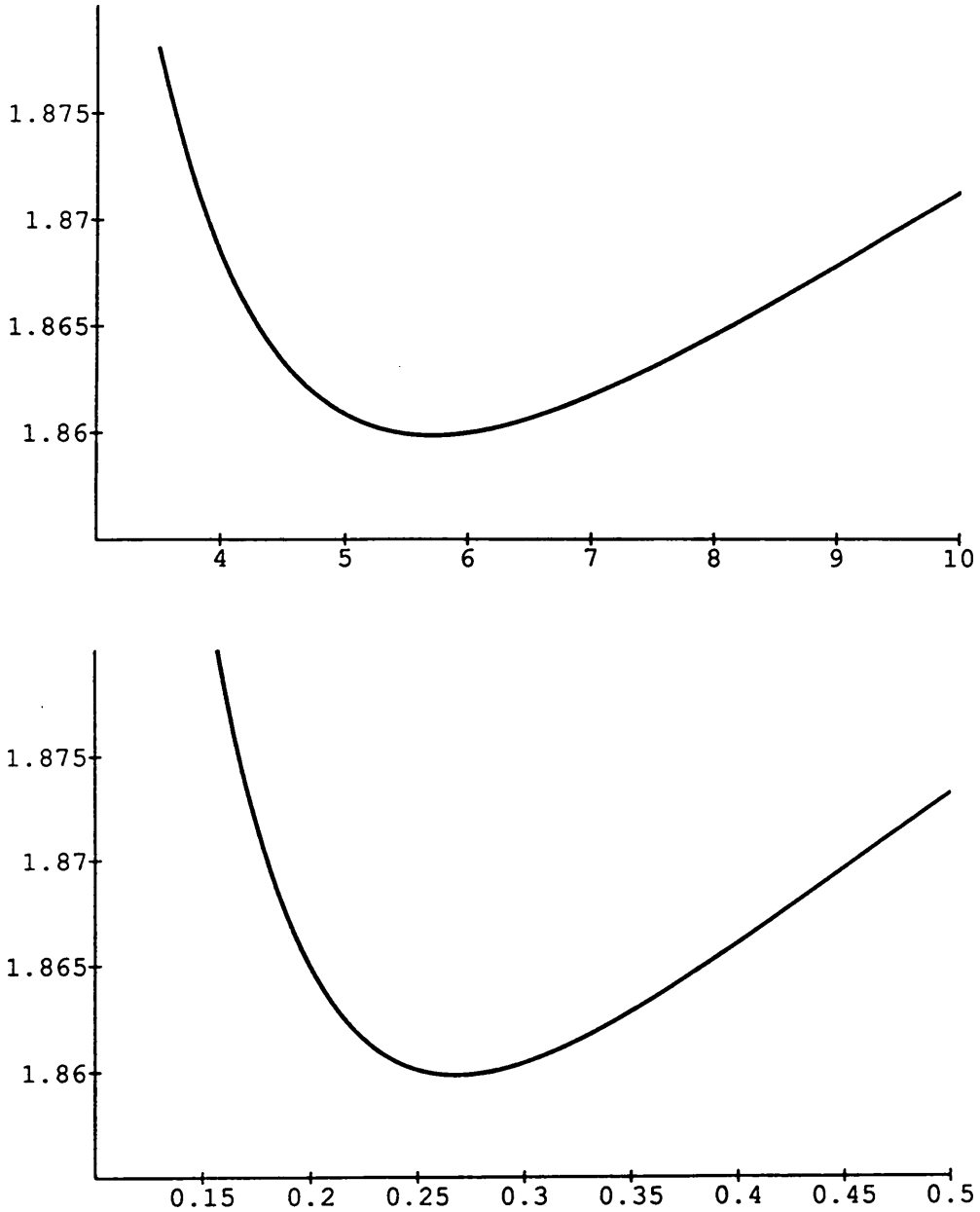

Figure 1: $f_1/[\mathrm{GeV}^{1/\gamma_{\mathrm{tr}}^2}]$ vs. $E_0/[\mathrm{GeV}]$ and $f_2/[\mathrm{GeV}^{1/\gamma_{\mathrm{tr}}^2}]$ vs. $B_z/[\mathrm{T}]$ for protons in the PS.

As for the "standard creed", it is easily demonstrated that $E_0 = E_{\mathrm{nom}}$ satisfies equation (9). That is, equation (3) provides one of the pair of solutions for the synchronous energy. In addition, substituting the time-derivative of this solution into equation (8), one finds that the corresponding synchronous phase is given by equation (4) (neglecting the betatron acceleration term).

3 MIXTURES OF IONS IN THE PS

3.1 An Open-loop Analysis

The acceleration of particles other than protons (or antiprotons) requires the modification of the RF frequency programme to cater for different charge-to-mass ratios. In the PS, this is achieved by the introduction, on a cycle-to-cycle basis, of a rate multiplication factor, b, which modifies the so-called B-train measurement of the dipole magnetic field. Thus, in the absence of feedback, the RF frequency would be generated as a slightly modified form of equation (2), viz.,

$$\omega_{\mathrm{RF}}(B_z;\, b) = \frac{hc}{R_{\mathrm{nom}}}\left[1 + \left(\frac{E_{\mathrm{rest,p}}}{q_{\mathrm{p}} b B_z \rho_{\mathrm{nom}} c}\right)^2\right]^{-1/2} \tag{10}$$

with, ideally,

$$b = \frac{q_{\mathrm{ion}}/E_{\mathrm{rest,ion}}}{q_{\mathrm{p}}/E_{\mathrm{rest,p}}}$$

Consequently, equation (6) becomes

$$f_1(E_0;\ \mathrm{ion}) = f_2(B_z;\, b) \tag{11}$$

where

$$f_1(E_0;\ \mathrm{ion}) = q_{\mathrm{ion}}^{-1/\gamma_{\mathrm{tr}}^2} E_0 (E_0^2 - E_{\mathrm{rest,ion}}^2)^{-(1-1/\gamma_{\mathrm{tr}}^2)/2} \tag{12}$$

is determined by ion species and

$$f_2(B_z;\, b) = (B_z \rho_{\mathrm{nom}} c)^{1/\gamma_{\mathrm{tr}}^2}\left[1 + \left(\frac{E_{\mathrm{rest,p}}}{q_{\mathrm{p}} b B_z \rho_{\mathrm{nom}} c}\right)^2\right]^{1/2} \tag{13}$$

is a function only of the free variable B_z.

Furthermore, since the graphical nature of the solution of equation (11) reveals that

$$\frac{dE_0}{dt} = \frac{df_2/dt}{df_1/dE_0} = \frac{dB_z}{dt}\,\frac{df_2/dB_z}{df_1/dE_0}$$

the synchronous phase is given by

$$\sin\varphi_0(B_z;\ \mathrm{ion},b) = \frac{2\pi R_{\mathrm{nom}}}{q_{\mathrm{ion}} \hat{V}_{\mathrm{RF}} c}\left[1 + \left(\frac{E_{\mathrm{rest,p}}}{q_{\mathrm{p}} b B_z \rho_{\mathrm{nom}} c}\right)^2\right]^{1/2} \frac{dB_z}{dt}\,\frac{f_2'(B_z;\, b)}{f_1'(E_0;\ \mathrm{ion})} \tag{14}$$

from equation (8). It should be noted that this form is only convenient when γ_{tr} is invariant and hence the total derivatives of f_1 and f_2 are the same as the partial ones.

Equations (11) and (14) provide the synchronous energy and phase, respectively, for a given ion species under open-loop conditions. That is, the RF frequency of equation (10) is not considered to be influenced by feedback. However, it is a strength of the approach developed thus far that this frequency is not assumed to be ideal, so that b, although a fixed parameter, may be chosen freely.

3.1.1 Oxygen and Sulphur

Since the value of b is close to one half for both $^{16}O^{8+}$ and $^{32}S^{16+}$, then, from equation (13), the f_2 curves for these ions are very similar. However, figure 2 shows that the different rest-mass energies of oxygen and sulphur are reflected in the corresponding f_1 curves. There is also a more subtle difference between the curves of figure 2 which is revealed by replotting f_1 as a function of $\gamma_0 = E_0/E_{\mathrm{rest,ion}}$ in the region near $\gamma_0 = \gamma_{\mathrm{tr}}$, as in figure 3. The minimum of the f_1 (and f_2) curve for sulphur lies below that of the one for oxygen. This fact is crucial to the arguments which follow.

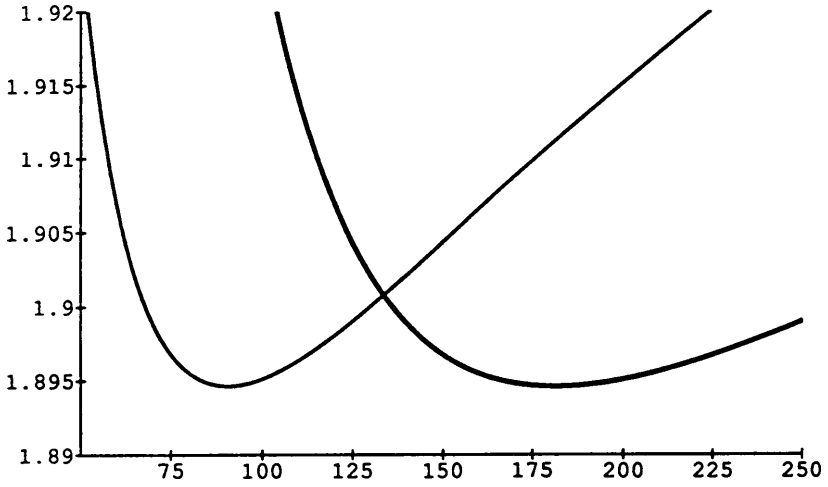

Figure 2: $f_1/[\mathrm{GeV}^{1/\gamma_{\mathrm{tr}}^2}]$ vs. $E_0/[\mathrm{GeV}]$ for $^{16}O^{8+}$ (thin line) and $^{32}S^{16+}$ (thick line) ions in the PS.

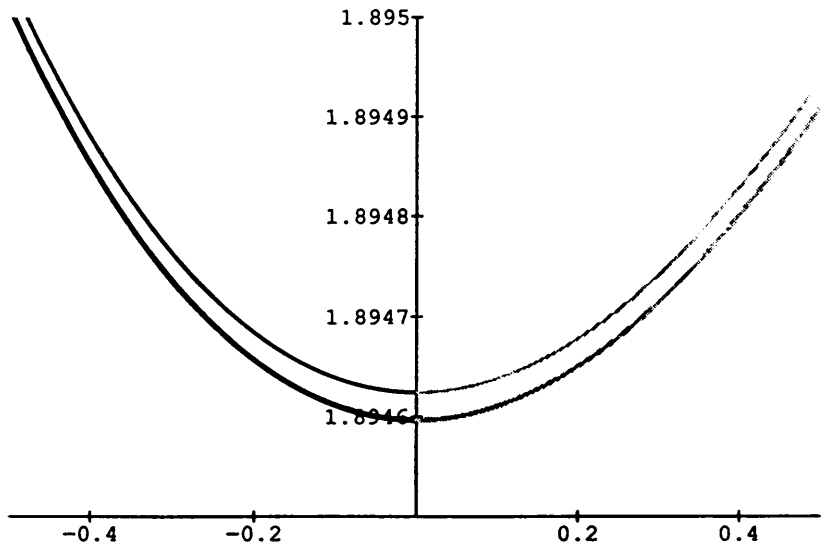

Figure 3: $f_1/[\mathrm{GeV}^{1/\gamma_{\mathrm{tr}}^2}]$ vs. $(\gamma_0 - \gamma_{\mathrm{tr}})$ for $^{16}O^{8+}$ (thin line) and $^{32}S^{16+}$ (thick line) ions in the PS. (Shading is used to emphasize that these curves span transition. The same distinction is made in all subsequent plots.)

The stage is now set for the (numerical) solution of equation (11), both above and below transition, for the various permutations of ion species and b. The result is shown in figure 4, first in the case when b is calculated for oxygen and then in the case when the RF frequency

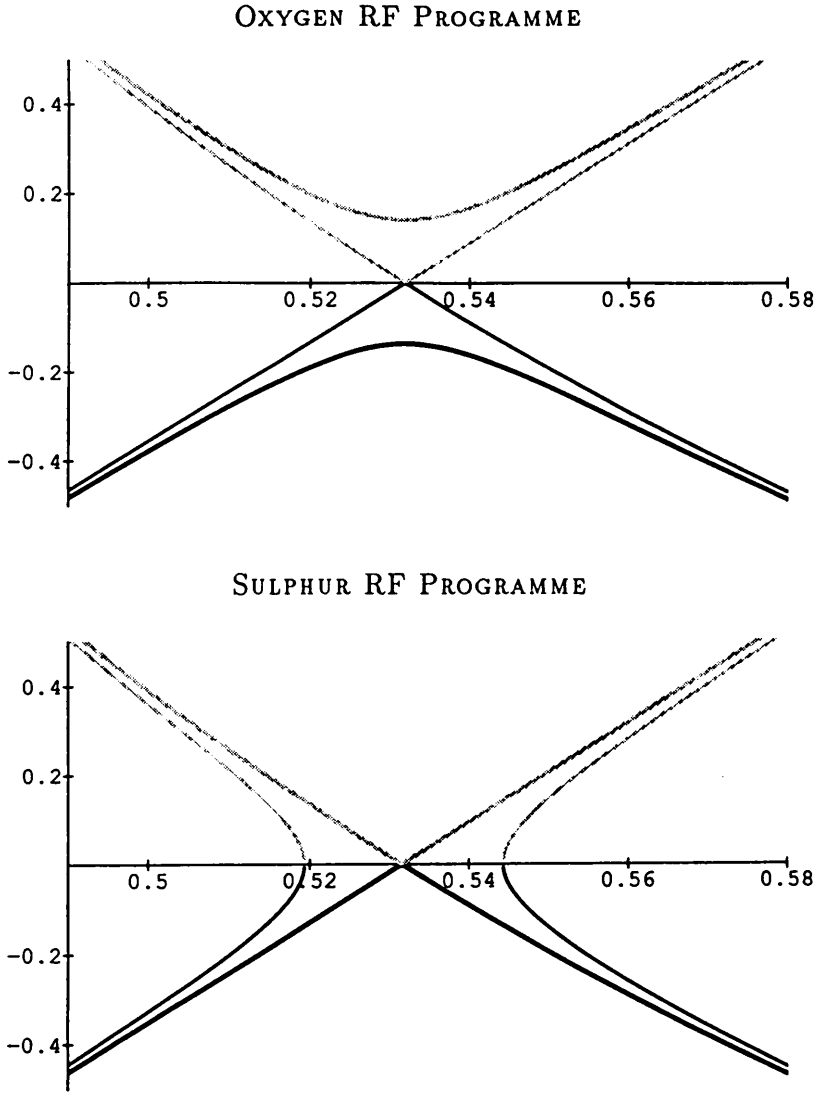

Figure 4: $(\gamma_0 - \gamma_{tr})$ vs. $B_z/[\mathrm{T}]$ for $^{16}O^{8+}$ (thin lines) and $^{32}S^{16+}$ (thick lines) ions in the PS. (Dark/light lines correspond to synchronous particles which are below/above transition.)

programme for sulphur is chosen. Both cases exhibit a monotonically increasing solution for γ_0 as a function of B_z for the ion species which corresponds to the RF programme; this is the "standard creed". There is also a decelerating solution for that species. However, for the other species, the solutions in the two cases are very different. For sulphur ions on the oxygen programme, the synchronous energy solutions above and below transition never meet. While for oxygen ions on the sulphur programme, there is a period of some 250 gauss during which there is no solution for the synchronous energy! These are consequences of the separation of the minima of figure 3. When the synchronous particle for oxygen crosses transition on its own RF programme, the value of $f_2(B_z)$ still lies above the minimum of the f_1 curve for sulphur and the two corresponding solutions for the synchronous energy for sulphur have their closest approach. Whereas, before the synchronous particle for sulphur reaches transition on its RF programme, $f_2(B_z)$ falls below the minimum of the f_1 curve for oxygen and there are no roots of equation (11) for oxygen ions.

The (scaled) synchronous energy solutions plotted in figure 4 are readily converted to the corresponding mean orbital radii using equation (5). The result is shown in figure 5, again for the two

different RF frequency programmes. In accordance with the "standard creed", both cases exhibit a synchronous particle which lies exactly on the central orbit for the ion species which corresponds to the RF programme. While the synchronous particle for the decelerating solution for that species plummets radially inwards. For sulphur ions on the oxygen programme, the synchronous particle orbit (approaching transition from below) duly heads towards the inside of the machine. However, at the point when oxygen reaches transition, this radial excursion for sulphur is no greater than that of the one in the opposite direction for oxygen on the sulphur programme. Thus, the "symmetry" of the radial separation persists, albeit qualified by the disappearance of the synchronous particle for oxygen as soon as it reaches transition on the sulphur programme.

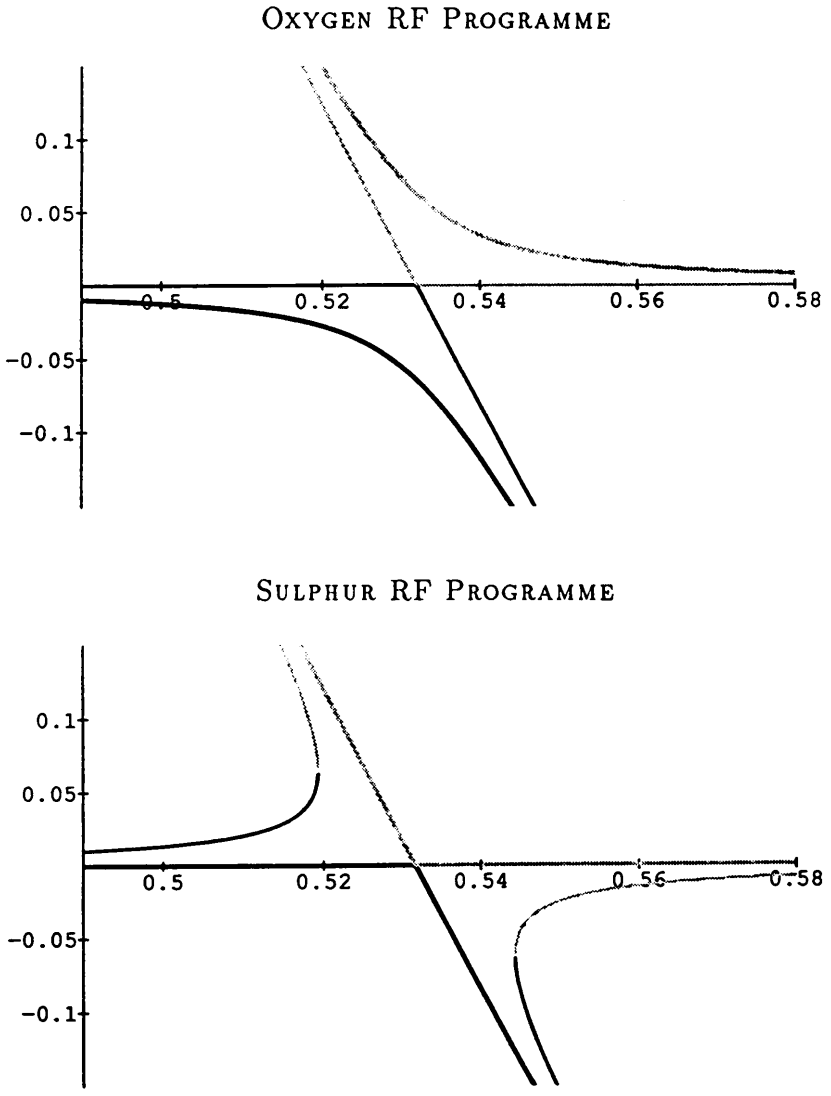

Figure 5: $(R_0 - R_{\mathrm{nom}})/[\mathrm{m}]$ vs. $B_z/[\mathrm{T}]$ for $^{16}O^{8+}$ (thin lines) and $^{32}S^{16+}$ (thick lines) ions in the PS. (Dark/light lines correspond to synchronous particles which are below/above transition.)

It should be noted that the orbits of figure 5 remain finite and that the subject of adiabaticity has not even been broached. The speed at which transition is approached does not affect these orbits. A synchronous particle is oblivious of the fact that, near transition, the aspect ratio of its RF bucket is changing too rapidly for the real particles to follow (because the synchrotron motion

of those particles is stagnating). Nor, for example, is the synchronous particle for sulphur on the oxygen programme aware of the distortion of the oxygen bucket as its oxygen counterpart crosses transition. It is, therefore, erroneous to attempt to describe the behaviour of the centre of motion of the sulphur ions in terms of an effective relative momentum defect with respect to the synchronous particle of oxygen. Rather, this momentum defect should only be used to predict the sign of the radial excursion made by one ion species on the RF programme of another. Thus, there is a *non sequitur* in the reasoning outlined in section 1.

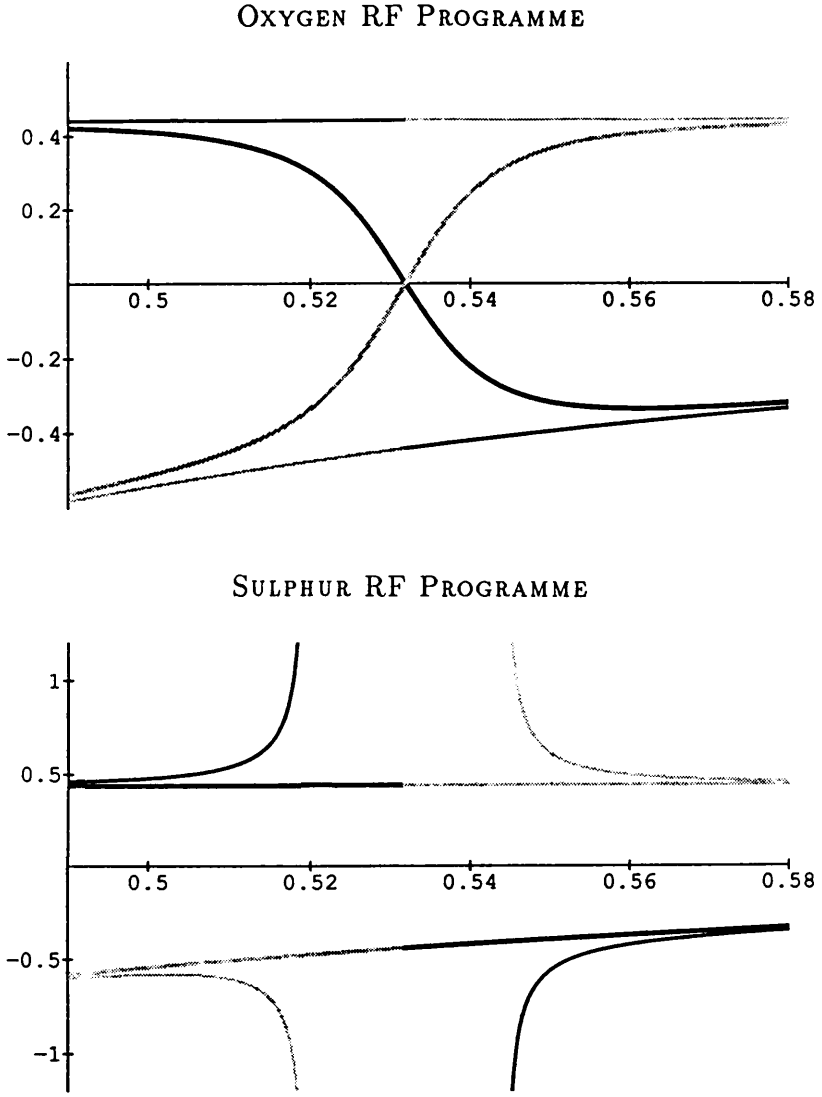

Figure 6: $\sin\varphi_0$ vs. $B_z/[\mathrm{T}]$ for $^{16}O^{8+}$ (thin lines) and $^{32}S^{16+}$ (thick lines) ions in the PS. (Dark/light lines correspond to synchronous particles which are below/above transition.)

The picture is completed by figure 6, which shows the solutions of equation (14) for the two RF programmes. For the purpose of illustration, I have simply taken constant values of $\hat{V}_{\mathrm{RF}}$ and dB_z/dt which are representative of the PS cycle for ions. Consequently, the accelerating synchronous phase for the ion species which corresponds to the RF programme is also constant; this is the "standard creed" of equation (4). However, at transition, the synchronous phase for that species is not defined because $f_1' = f_2' = 0$, albeit instantaneously. Thus, although the accelerating and decelerating

synchronous energy solutions meet at transition for the ion species which corresponds to the RF programme, there is a discontinuity in the corresponding synchronous phases at this point.

Turning to the synchronous phase for the ion species which does not correspond to the RF frequency programme, the solutions in the two cases are again very different. For sulphur ions on the oxygen programme, the sine of the synchronous phase is zero when oxygen crosses transition (here, the sulphur solutions below and above transition are 180° apart). While for oxygen ions on the sulphur programme, the synchronous phase becomes imaginary and the oxygen bucket collapses even before the solution for the synchronous energy disappears.

The response of a phase loop to this longitudinal separation of the two species would depend upon their contributions to the total beam current. If the beam were dominated by its oxygen content, sulphur ions accelerated on the oxygen programme would head off towards 0° largely unnoticed. Then, even if the sulphur were not completely eliminated against the beam pipe, any surviving ions would find themselves at an unstable phase well below transition and on the opposite side of the vacuum chamber to the RF bucket which could support them above transition when the transition phase jump occurred. However, any migration of oxygen ions towards 90° on the sulphur programme would be opposed by the phase loop. Then, depending upon the gain and time-constant of the loop, the sulphur programme would tend to be made to resemble the oxygen one. Thus, a mechanism has been found which could account for the difficulties that were experienced when it was required to remove the oxygen ions.

3.2 Experimental Observations

It is an important prediction of the previous section that $^{16}O^{8+}$ and $^{32}S^{16+}$ ions will separate longitudinally near transition. This is indeed observed. Figure 7 shows a series of longitudinal beam profile measurements that was obtained using a fast, resistive-wall pick-up when the RF system of the PS had been optimized for oxygen. These measurements were triggered by the RF at times successively closer to the transition phase jump, the last profile being triggered 5 ms later than the first (although, necessarily, on a different cycle). The appearance of a second, much less intense bunch at earlier times with respect to the trigger may now be interpreted as the sulphur ions heading towards 0° with respect to the zero-crossing of the RF. However, it must be stated that this interpretation is experimentally corroborated only by the observation of similar proportions of the two ion species in spectrometry measurements at the source.

A very similar series of longitudinal profiles is shown in figure 8, but, in this case, the RF system had been optimized for sulphur. The inference from the previous section is that, here, although the oxygen ions would like to take off towards 90°, they are prevented from doing so by the action of the RF phase loop which is, however, almost blind to the presence of the sulphur. Thus, the net result of the expected longitudinal separation is the displacement of the sulphur ions to lower phase with respect to the zero-crossing of the RF.

An additional feature of figure 8 is that, in the last three frames, the oxygen progressively debunches. Since the oxygen arrives at transition before the transition phase jump occurs on the sulphur programme, this may be due simply to the unstable motion of the higher energy oxygen ions which cross transition ahead of their colleagues. However, it could be indicative of the collapse of the oxygen bucket as the synchronous particle for oxygen reaches transition.

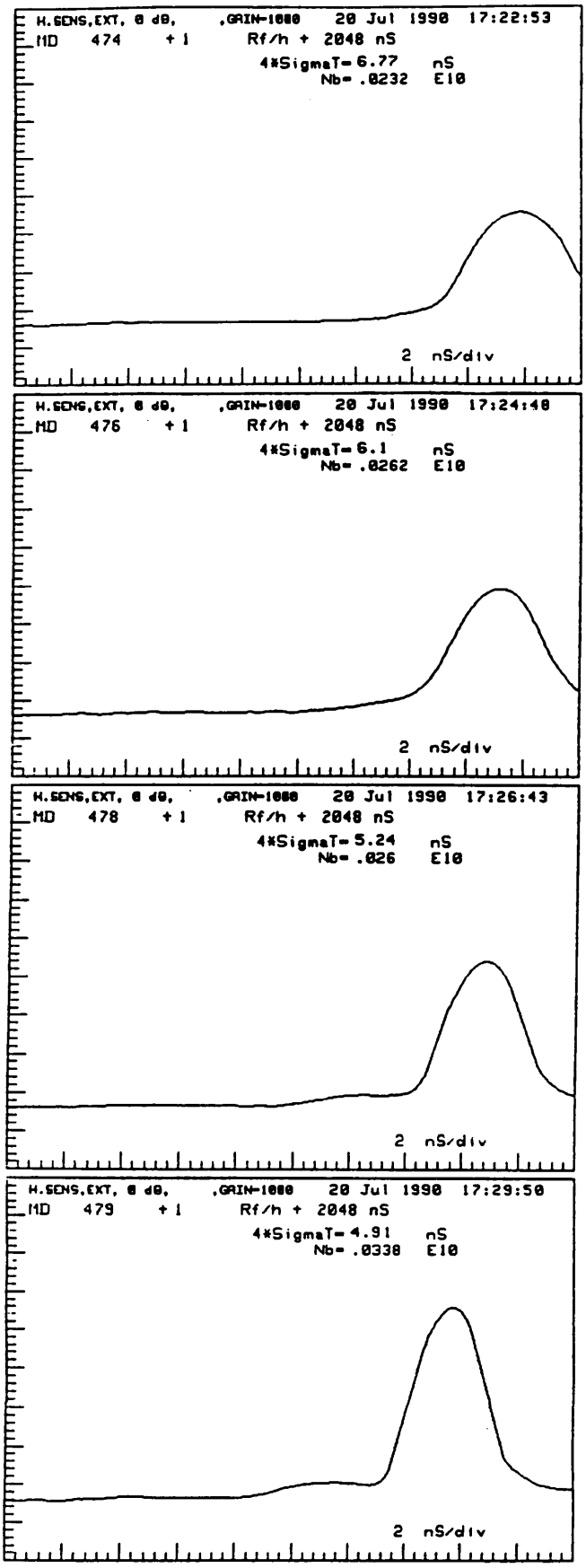

Figure 7: Longitudinal beam profiles taken on the RF programme for oxygen.

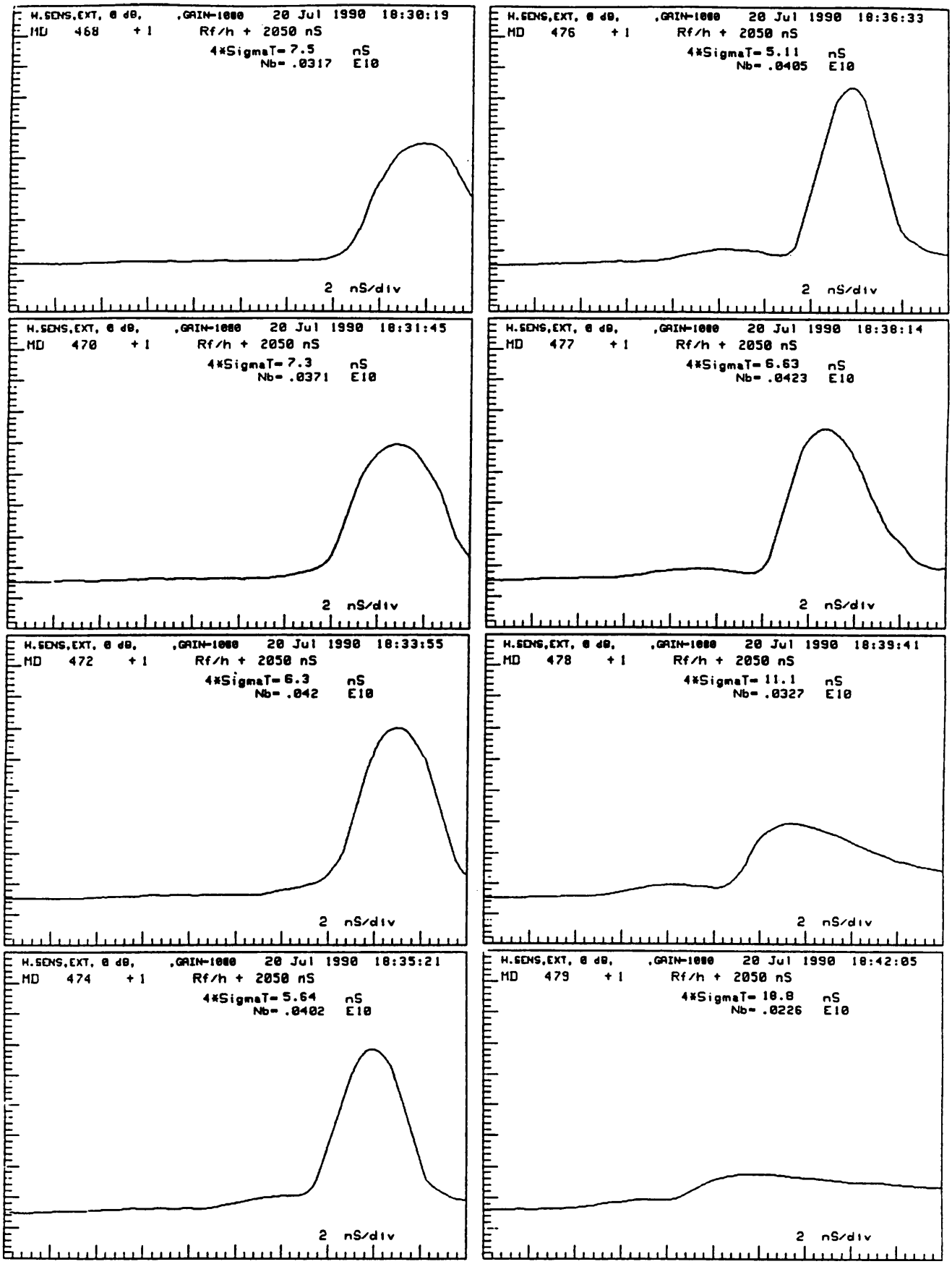

Figure 8: Longitudinal beam profiles taken on the RF programme for sulphur.

The radial separation of the two species is also observed. Figure 9 shows a horizontal beam profile measurement that was obtained using a flying-wire scanner when the RF system had been optimized for sulphur. The timing of this measurement corresponds approximately to that of the fourth frame of figure 8, but such a scan is made over many turns and is not a "snapshot" of a single bunch. The dominant profile appears at larger radial position and may be identified as the oxygen. Significantly, the sulphur lies inside the central orbit, apparently having been displaced by the action of the phase loop. Operationally, a perturbation is added to the RF phase programme to counteract this effect. Without the perturbation, the oxygen ions do not reach the aperture limit of the machine; they survive, but only to debunch upon crossing transition, as in figure 8. The debunching beam is observed with the flying-wire to spread across the entire vacuum chamber and, evidently, this assures that some oxygen ions find their way into the bucket which can support them above transition.

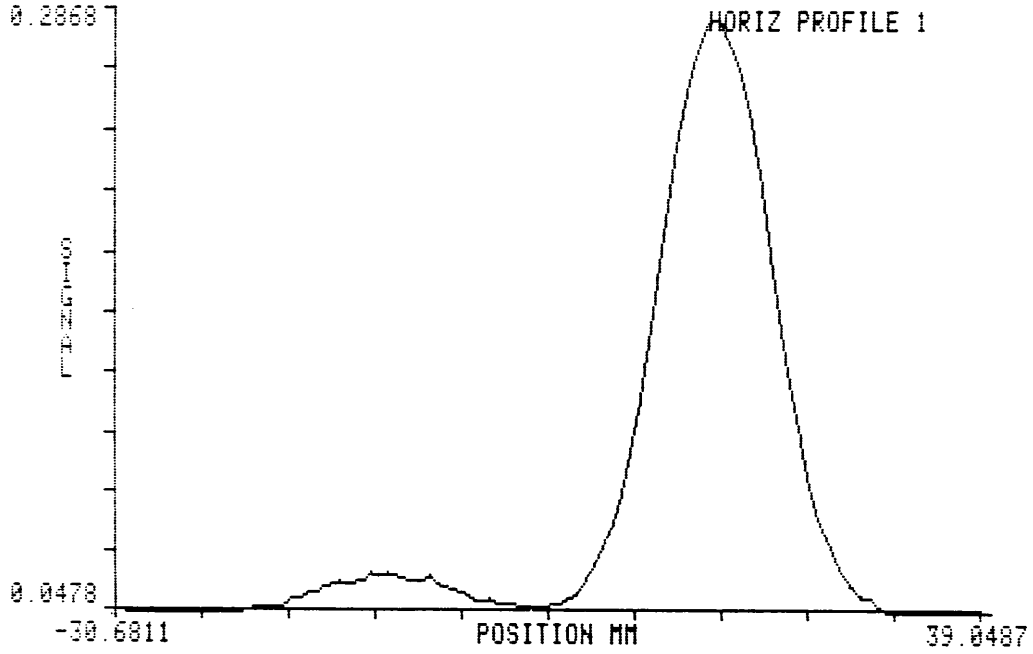

Figure 9: Horizontal beam profile taken on the RF programme for sulphur. The centre of the aperture corresponds to a measured position of zero.

A similar picture to figure 9 is obtained when the RF system is optimized for oxygen, except that the oxygen profile remains closer to the centre of the aperture while the one for sulphur heads towards the inside of the machine. Operationally, no phase perturbation is required to eliminate the sulphur ions.

Despite the fact that the RF frequency programme of the PS is sufficiently accurate to permit open-loop acceleration without loss (up to transition), the above measurements are made meaningless in such conditions by the violent dipolar bunch oscillations which result from the quantized measurement of the magnetic field. This has precluded a quantitative test of the theory.

4 CONCLUSIONS

A remarkably simple derivation has been developed which yields the synchronous particle parameters without the tacit assumption of an idealized RF frequency. However, the simplicity is a

consequence of treating the momentum compaction factor as independent of radial position, which, without further refinement of the theory, may limit its range of application.

Where they may be compared, the results obtained are entirely in agreement with those of more familiar derivations, except that a second synchronous particle is revealed on the other side of transition. I see no reason to dismiss this synchronous partner as a mere artefact of the theory. However, since it appears inside the vacuum chamber only fleetingly near transition, there is no obvious test of its existence. A more tangible prediction is the separation, both radially and longitudinally, of oxygen and sulphur ions as they approach transition. These effects have been observed in the PS and it is the latter which explains why the dominant species is more difficult to eliminate from the mixture.

It would be interesting to compare the experimental results with those of a computer model, but this would require a longitudinal phase space tracking code based upon difference equations that can handle mixtures of particles and simulate AC-coupled RF feedback.

Acknowledgements

I am enormously indebted to Roland Garoby, whose interest, assistance and encouragement at the formative stages of this work were unique. I am also grateful to all those who were prepared to listen to me rant on the subject or who provided comments once these ideas had been drafted.

Distribution (of abstract)
PS, SL, AT and MT Scientific Staff